

A three-layered sphere model of the optical properties of phytoplankton

James C. Kitchen and J. Ronald V. Zaneveld

College of Oceanography, Oregon State University, Corvallis 97331

Abstract

Theoretical scattering computations are performed on a phytoplankton model consisting of three concentric spheres. The outer sphere represents the wall, membrane, or frustule and is assigned a relatively high index of refraction with no absorption. The middle layer represents the chloroplasts and is assigned a relatively low index of refraction with absorption. The core represents the balance of the cytoplasm and is given a low index of refraction with no absorption. The model is applied to an observed size distribution from the Pacific central gyre. This model produced significantly more backscattering and attenuation than a low-index, homogeneous-sphere model. Changing the distribution of cell-wall thickness as a function of particle size produces much variation in the shape of the volume scattering function.

The major tool for the global study of oceanic properties is remote sensing by either passive sensing of ocean color or by active LIDAR. In either case, interpretation of the remotely sensed data depends on understanding the inherent optical properties, especially backscattering. Radiative transfer models (see Gordon and Morel 1983) contain parameters of the form $F_{L\beta} b_b/a$, where $F_{L\beta}$ is a parameter that depends on the radiance distribution and the volume scattering function, $\beta(\theta)$, of the water and particles. b_b is the backscattering coefficient and a is the absorption coefficient. The remotely sensed data thus depend primarily on absorption and backscattering (Gordon and Morel 1983).

The models currently used to obtain backscattering from remotely sensed data assume that for case 1 waters (Morel and Prieur 1977) the backscattering, biomass, and absorption can be described as being dependent only on the chlorophyll concentration (Gordon et al. 1988; Platt et al. 1988; Morel 1988). Although the statistical dependence of backscattering and absorption on chlorophyll concentration is extremely

useful in the inversion of remotely sensed ocean color spectra, we have shown (Kitchen and Zaneveld 1990) that these relationships cannot be used to predict the vertical structure of scattering and backscattering as a function of vertical chlorophyll structure. Thus, we need a better understanding of the relationship of volume scattering functions and the biological properties of particles suspended in the ocean.

Two decades ago researchers applied Mie (1908) scattering theory to combinations of high-index (mineral) and low-index (phytoplankton) particles to explain the observed inherent optical properties (Brown and Gordon 1973; Zaneveld et al. 1974). These methods could reproduce the inherent optical properties, but the results were not convincing in explaining the nature of the particles because they indicated a high percentage of high-index particles in regions dominated by phytoplankton. At the same time, Mueller (1974) used a three-layered-sphere model of phytoplankton to explore the sensitivity of remotely sensed color spectra to parameters other than chlorophyll content. However, he did not compare the results of his method to those of the component models, nor did he have enough sea-truth data to investigate the actual nature of the particles.

The results of the component models are not convincing and they have not found wide use in explaining the distribution of optical properties. Recent Mie scattering studies (e.g. Cohen et al. 1983; Latimer 1984) have

Acknowledgments

Support was provided by ONR (N00014-90-J-1132), DOE (SBIR contract DE-AC03-89ER80788), and NSF (OCE 89-11355). Sea Tech, Inc., supported part of the work through in-house research funds.

James L. Mueller provided the Fortran code for the Mie subroutines. We also thank Annick Bricaud for suggestions.

concentrated on odd shapes and structures that have been too complicated (or applicable only to a small percentage of the particles present) for use on natural assemblages of phytoplankton. Likewise, Meyer (1979) has shown the effect of thin membranes on the volume scattering functions of several monosized particles. Quinby-Hunt et al. (1989) have used the coated-sphere model to explain the observed scattering matrix of a culture of *Chlorella* picoplankton. We will use the Mie scattering of three-layered spheres to examine the interaction of particle size distribution, cell-wall thickness, the proximity of the chloroplasts to the surface, and the inherent optical properties of natural particles in water.

Although knowledge of the backscattering coefficient is important in the interpretation of remotely sensed data in the visible part of the spectrum, very few measurements have been made. Petzold (1972) carried out measurements of the volume scattering function in situ at one or two wavelengths that included backscattering measurements and Downing et al. (1981) measured backscattering in very turbid waters. Moore et al. (unpubl. rep.) developed a backscattering device that operates in the IR at 880 nm. Sea Tech, Inc., and the Johns Hopkins University/APL have developed backscattering sensors that operate in the blue part of the spectrum (unpubl. rep.). Few of the backscattering studies include simultaneous measurements of chlorophyll. Thus we have few data to describe the distribution of backscattering in the ocean.

The three-layered-sphere model

We have chosen to model phytoplankton as three-layered spheres (Fig. 1). The outer layer represents the cell membrane, wall, or frustule. We have assumed this layer to be nonabsorbing and to have an index of refraction equal to 1.09 relative to seawater, which is consistent with most organic oils and waxes and with amorphous silica (Mueller 1974). A coccolithophore with a carbonate shell might have an index of 1.15–1.20. The second layer represents the chloroplasts to which we have assigned an index of refraction of $1.02 - in'$. The imaginary

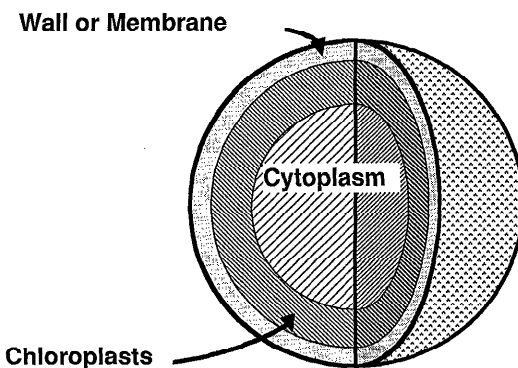


Fig. 1. The three-layered-sphere model of phytoplankton structure.

part of the index of refraction, n' , is proportional to the absorption coefficient, γ , of the substance, and the relationship is given by

$$n' = \gamma\lambda/4\pi.$$

Thus, the imaginary part of the index of refraction was chosen to be proportional to the chlorophyll concentration in the chloroplast layer. For our computations, we adjusted the values (at 660 nm) for a combination of phytoplankton pigments given by Mueller (1974) to agree with our intercellular concentrations of Chl *a*.

For our reference natural population, we used chlorophyll concentrations, size distributions, and attenuation coefficients found at the chlorophyll maximum in the central gyre of the Pacific Ocean in October–November 1982 (Kitchen and Zaneveld 1990). We used a wavelength of 660 nm to match the wavelength of our transmissometer during that cruise. Extrapolating our observed size distribution to cover the range $0.25 < r < 15.0 \mu\text{m}$, we observed intercellular chlorophyll concentrations of $1.87 \times 10^{-7} \text{ m}^3 \text{ mg}^{-1}$ which yielded $n' \approx 0.005$ at 660 nm if the pigment was confined inside a $0.2\text{-}\mu\text{m}$ outer shell (two-layer model). If a core of nonpigmented cytoplasm exists, it has been assigned an index of 1.02 with no absorption component, and n' for the middle (chloroplast) layer is adjusted by the inverse of the ratio of its volume to the volume of the core plus the middle layer. For example, if the inner radius of the middle

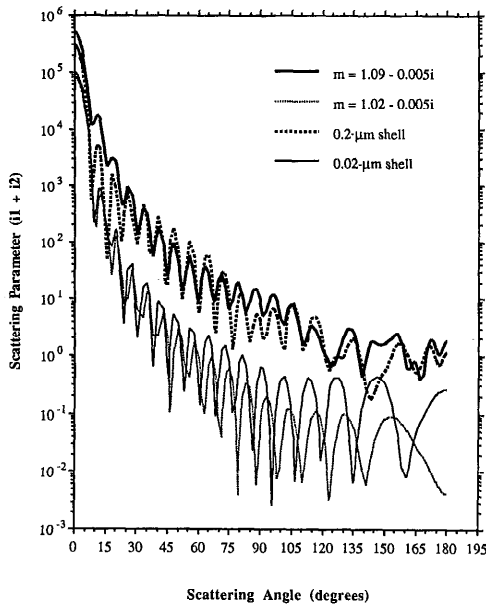


Fig. 2. A comparison of the volume scattering functions for monosized ($r = 2 \mu\text{m}$) two-layered spheres with those obtained for homogeneous particles.

layer is 80% of the outer radius of the middle layer, then

$$n' = 0.005 / (1 - 0.8^3) = 0.010$$

if the shell remains $0.2 \mu\text{m}$ thick. This calculation keeps the amount of chlorophyll per cell constant from model to model.

The physical properties of the cell (outer radius, r_3 ; inner radius of wall or membrane, r_2 ; inner radius of chloroplasts, r_1 ; pigment content, $\sim n'$) vary a great deal in nature; we know of no studies that would aid us in assigning a size distribution to these parameters. The indices of refraction are themselves questionable. Aas (1981) reported indices for silica as 1.045–1.067, calcite as 1.18–1.25, and, surprisingly, pigments as 1.12. Charney and Brackett (1961) reported the indices of refraction for cytoplasm to be 1.015, for the chloroplasts to be 1.06, and for cell membranes (*Chlorella*) to be only 1.02. There is thus considerable uncertainty regarding essentially all the parameters of the model. However, this uncertainty does not negate our purpose here, which is to demonstrate that we can model these struc-

tural parameters and determine their importance in scattering calculations.

The exact solution to the electromagnetic field equations for light scattering by a spherical particle was derived by Mie (1908), and this type of scattering has been dubbed "Mie scattering." Our programs for numerical computation of the Mie solution extended to three-layered spheres followed the techniques of Kerker (1969) and Mueller (1974). The results of a few test cases were compared with those resulting from use of the algorithms of Bohren and Huffman (1983) for homogeneous and two-layered spheres. We found no significant differences.

Volume scattering functions of monosized particles—The volume scattering functions of particles with a $2.0\text{-}\mu\text{m}$ radius and either a 0.02- or $0.2\text{-}\mu\text{m}$ cell wall (two-layered sphere) are compared to the scattering function of homogeneous particles with the same radius (Fig. 2). The two-layered spheres have been assigned indices of refraction of $1.02 - 0.005i$ and $1.09 - 0.005i$ for the inner and outer layers respectively. The indices of refraction relative to seawater were $1.02 - 0.005i$ and $1.09 - 0.005i$ for the "soft" and the "hard" homogeneous spheres. The volume scattering function of the coated sphere with the $0.2\text{-}\mu\text{m}$ shell is similar to that of the higher index particle beyond 25° but is not at all similar to the low-index uniform particle. The particle with the $0.02\text{-}\mu\text{m}$ shell is similar to the low-index particle from 0 to 60° . Beyond 60° , the thin-shelled particle scatters more than the low-index particle, with about an order of magnitude difference beyond 120° . The differences were even more pronounced for particles with a radius of $4.0 \mu\text{m}$ (not shown).

Cumulative attenuation, scattering, and absorption coefficients (with respect to particle size)—The results of the Mie scattering computations for 55 different particle sizes were combined in the proportions indicated by a two-segment, power-law fit to the particle size distribution observed for the chlorophyll maximum in the Pacific central gyre in October and November 1982 (Kitchen and Zaneveld 1990). The observed size distribution ($1\text{--}7.5\text{-}\mu\text{m}$ radius) was fitted by a

segmented power relationship

$$dN = N_0 D^{-s} dD \quad (1)$$

with an exponent (s) of 3.63 for particles $< 3.3\text{-}\mu\text{m}$ radius and $s = 4.96$ for particles $> 3.3\text{-}\mu\text{m}$ radius. The imaginary part of the indices of refraction were chosen to be consistent with the observed ratios of chlorophyll to particle volume, assuming the observed particle size distribution to be extrapolated to cover the range $0.25\ \mu\text{m} < r < 15.0\ \mu\text{m}$. Bacteria $< 0.20\ \mu\text{m}$ in radius are unlikely to contribute to optical properties due to their very low optical efficiencies. Stramski and Kiefer (1991) concluded that the bulk of backscattering is from detrital particles in the range of $0.2\text{--}0.5\text{-}\mu\text{m}$ radius, assuming a uniform power-law size distribution with $s = 4.0$. We did not carry out Mie calculations for radii $< 0.3\ \mu\text{m}$ because they failed to converge in the constant shell-thickness models.

The main reason that we used an observed natural size distribution is that we found it difficult to relate results shown elsewhere for monosized particles or narrow size distributions to natural conditions. The concentrations of submicron particles were not measured by the particle counter. We do not claim, therefore, that our extrapolation necessarily represents the actual concentrations of the small particles. We were motivated to extend the size distribution to very small sizes to understand the importance of the various factors in nature. We are encouraged by the fact that our results do qualitatively resemble the observed optical properties.

The three-layered models have the pigment confined to the middle layer of a three-layered sphere. For all three-layered models the inner radius of the middle layer is 80% of the outer radius of the middle layer. The imaginary part of the refractive index is adjusted for each size particle by dividing by the ratio of its pigmented volume to the pigmented volume of a two-layered cell with a $0.2\text{-}\mu\text{m}$ cell wall and the entire center with a $-0.005i$ imaginary part for the refractive index. This adjustment is done to avoid shifting chlorophyll from one part of the size spectrum to another by changes in the in-

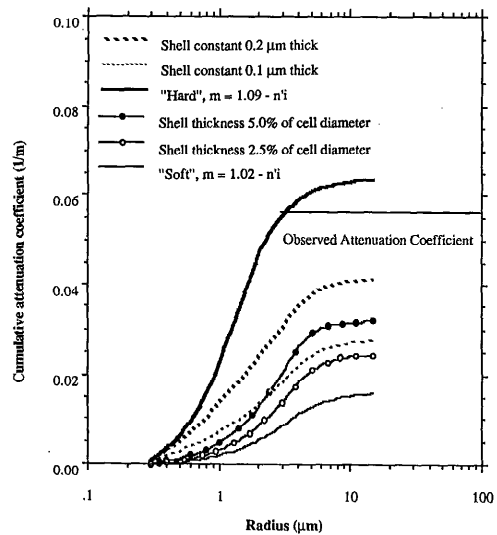


Fig. 3. The cumulative beam attenuation coefficients relative to particle radius for four three-layered models and two homogeneous models of phytoplankton.

ternal cell structure. As shown previously, this results in $n' = 0.010$ for three-layered models with a $0.2\text{-}\mu\text{m}$ shell. For shells with other thicknesses, n' will vary slightly from one size particle to another depending on how the thickness of the shell compresses or decompresses the pigmented volume. This variation in n' should not result in unrealistically high indices, because the most compacted chloroplasts are found in the small particles of the reference model. All other models produce lower complex components of the index of refraction for the small particles.

We present two models with a constant shell thickness and two with a shell thickness proportional to the particle radius. The former might represent species with thin membranes and the latter ones with cell walls or silica frustules. Figure 3 shows cumulative attenuation as a function of particle size for the various models. We see that a homogeneous "soft" particle ($m = 1.02 - 0.005i$) yields only 29% of the observed (Kitchen and Zaneveld 1990) attenuation while a homogeneous "hard" particle ($m = 1.09 - 0.005i$) yields 114% of the observed attenuation. The three-layered model with

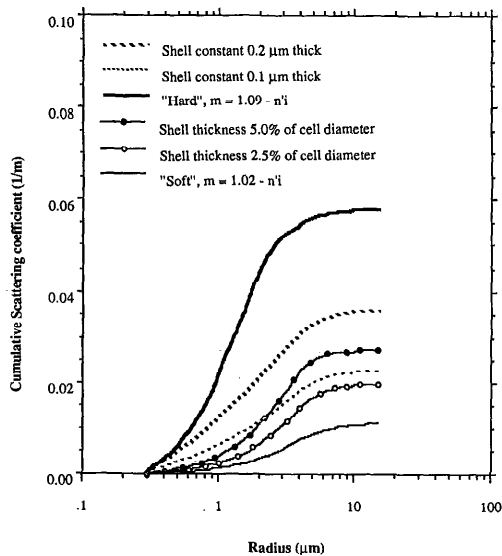


Fig. 4. As Fig. 3, but of the cumulative scattering coefficients.

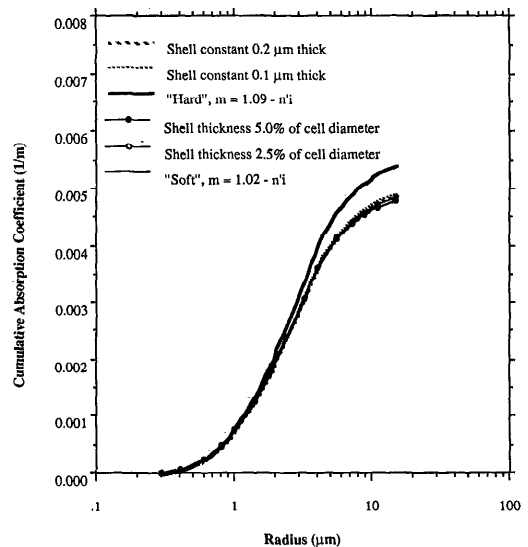


Fig. 5. As Fig. 3, but of the cumulative absorption coefficients.

a 0.2- μm shell yields 73%, and one with a shell thickness equal to 2.5% of the cell diameter yields 57% of the observed attenuation coefficient. Thus the three-layered model yields a first-order agreement with the observed attenuation that could not be obtained with a homogeneous soft-particle model of phytoplankton. Note that for the size distribution used, the $0.5 < r < 3.0$ - μm size fraction contributes the most to the attenuation. The $r < 0.5$ - μm size fraction also contributes to attenuation but at a reduced level. If the concentration of these small particles, $r < 0.5$ μm , greatly exceeds that predicted by the -3.66 power-law distribution, they could greatly influence total attenuation.

The plots of the cumulative scattering coefficients (Fig. 4) are very similar. Cumulative absorption (Fig. 5) reveals a much different behavior. The absorption is not very sensitive to the particle structure. All the models except the homogeneous hard particle vary $< 2.5\%$ in their absorption. The hard-particle model yields 14% more absorption, presumably because the light rays are not reflected off the inner surface of the wall but are refracted inward toward the chloroplasts.

Cumulative volume scattering function—

The cumulative (with respect to particle radius) volume scattering function at four angles for the constant 0.1- μm -shell model are shown in Fig. 6. Roughly 75% of the backscattering is due to particles < 2 μm in radius while the same percentage is not reached until 3–6 μm for forward scattering. Also note that particles > 15 μm would seem to contribute negligibly to the 3° , 161° , and 180° scattering for the observed particle size distribution, whereas contributions are still being made to the 0° scattering by 15- μm particles. The 0.2- μm -shell model (not shown) gives similar results except the 15- μm particles are still contributing slightly at 180° . The same plots for the 2.5% proportional shell model (Fig. 7) show a very large contribution by the 15- μm particles at 0° and 180° , negligible contribution at 3° , and a slight contribution at 161° . The 5.0% proportional shell model is similar. For the soft homogeneous model (Fig. 8), the 15- μm particles contribute only to the 0° scattering. The same is true for the hard homogeneous model.

Bacteria-sized particles ($r < 0.5$ μm) contribute negligibly to forward scattering but contribute strongly in the backscattering region. However, the dominance of backscattering by these particles, as suggested by

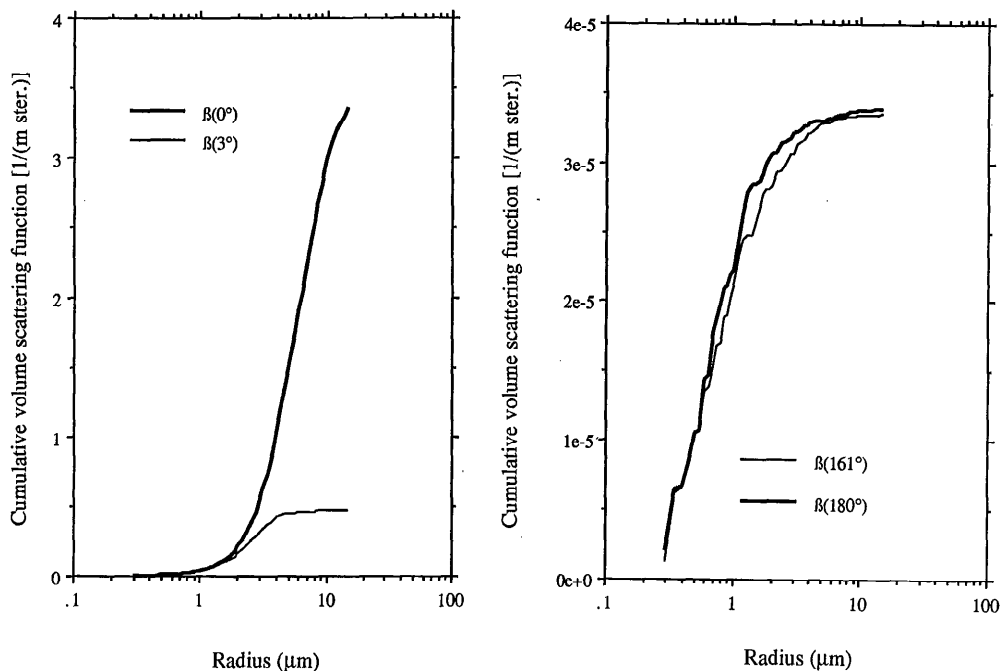


Fig. 6. The cumulative volume-scattering function at 0° and 3° and at 161° and 180° relative to particle radius for a polydispersion of three-layered spheres with $0.1\text{-}\mu\text{m}$ -thick outer shells. The size distribution matches that observed in the Pacific central gyre. The steplike features in this and other figures are due to the oscillatory nature of Mie coefficients, which would be smoothed in nature by the polydispersion of structures and indices.

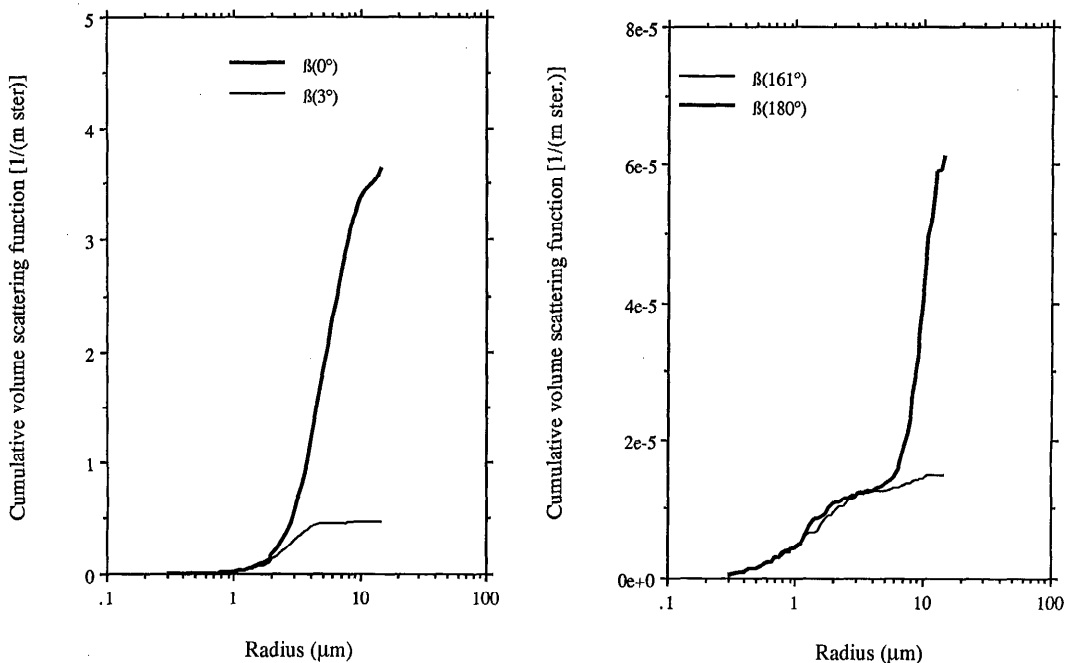


Fig. 7. As Fig. 6, but of three-layered spheres with outer shell thicknesses 2.5% of the cell radius. The size distribution matches that observed in the Pacific central gyre.

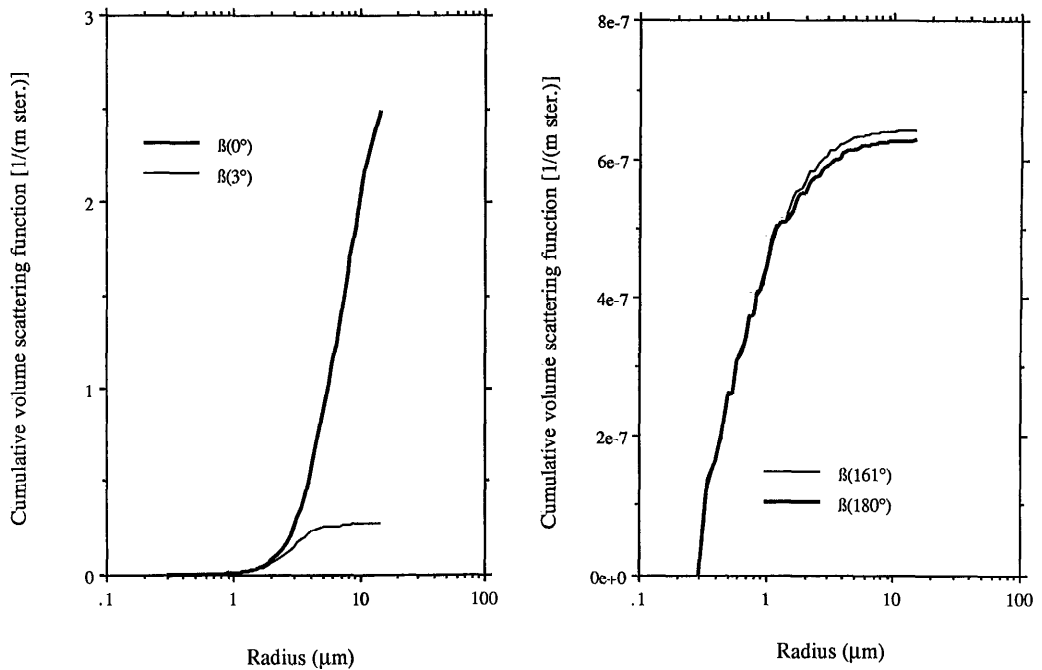


Fig. 8. As Fig. 6, but of homogeneous spheres with indices of refraction = $1.02 - mi$. The size distribution matches that observed in the Pacific central gyre.

Figs. 6 and 8, is unrealistic. In Fig. 6 (0.2- μm shell), particles in that size range would be mostly shell which is not a likely structure. In Fig. 8 (soft particles), total backscattering is two orders of magnitude less than that produced by the models with shells and thus would not be significant in a mixture of particles.

Volume scattering functions for various spherical models—The volume scattering functions of the proportional shell thickness (5%) and the constant shell thickness (0.2 μm) are compared with those for homogeneous spheres (hard $\rightarrow m = 1.09$; soft $\rightarrow m = 1.02$) in Fig. 9. All models are polydispersions based on the observed size distribution in the Pacific central gyre in October and November 1982. Some historical observations of particulate volume-scattering functions (Petzold 1972) from oligotrophic waters are also shown on Fig. 9. The three-layered-sphere models produced as much or more backscattering and near-forward scattering than the homogeneous hard sphere with a 1.09 real component of the index of

refraction. The soft sphere with a 1.02 real part of the index of refraction yielded two orders of magnitude less backscattering. It is also clear that both the homogeneous models give scattering functions that are too steeply sloped in the forward direction to yield the observed volume scattering function. The 0.2- μm -shell model, however, follows the volume scattering function from 0° to 90° very well.

The volume scattering functions for the four three-layered-sphere models are shown in Fig. 10. Various shapes are shown but the absolute magnitude at any angle varies less than an order of magnitude. The proportional-shell models exhibit enhanced 180° scattering due to the influence of the thick shells in the larger particles. The most striking difference is between the two models of constant shell thickness. The larger backscattering in the thin-shelled model is due to the smallest particles. Evidently the larger inside sphere resulting from the thinner shell contributes significantly to backscattering in the small particles. We see that

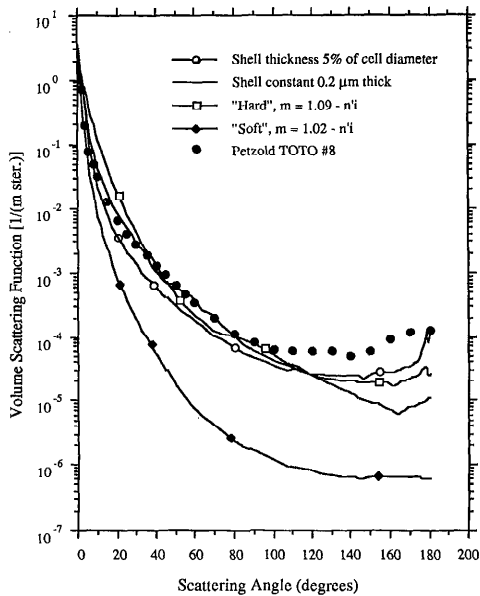


Fig. 9. A comparison of volume scattering functions for two three-layered-sphere polydispersions vs. those for high and low index-of-refraction homogeneous spheres. The size distributions match those observed in the Pacific central gyre. Also shown is a measured particulate volume-scattering function from the central gyre (Petzold 1972) obtained by subtracting scattering from seawater filtered for 18 h through diatomaceous earth from the observed scattering function.

variation in the internal structure of the phytoplankton models can produce much variation in the fine detail of the shape of the volume scattering function in both the forward and backscattering region, but relatively little change in the overall magnitude.

The fine detail of the backscattering (90° – 180°) is strongly influenced by particle shape (Gibbs 1978; Asano and Sato 1980)—a parameter not considered here. Gibbs (1978) showed an increased $\beta(180^{\circ})$ for his calculations on cubes and plates, while Asano and Sato (1980) showed that randomly oriented spheroidal shapes had less structure in backscattering than was exhibited by spheres. Deviation of the concentration of submicron particles (Morel and Ahn 1990; Stramski and Kiefer 1991) from that indicated by our extrapolation would also influence backscattering. Results for our model should thus be interpreted more cautiously

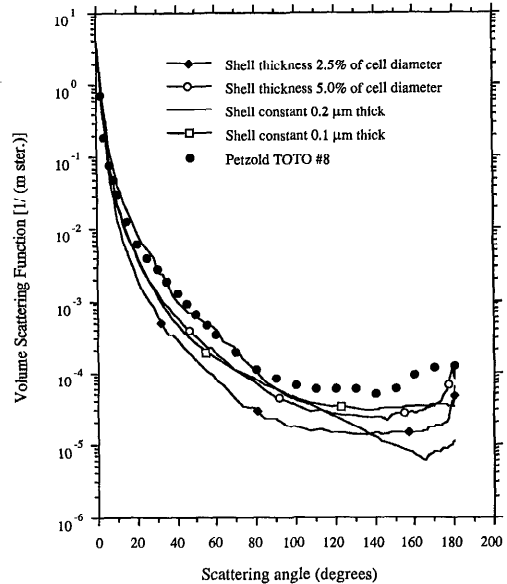


Fig. 10. As Fig. 9, but for four three-layered-sphere polydispersions showing the effect of changes in the wall-thickness distribution.

in the backscattering region than the results for forward scattering.

Particle size distribution effects on volume scattering functions—As stated earlier, the size distribution in the central gyre chlorophyll maximum was fitted by a segmented power relationship (Eq. 1) with an exponent (s) of 3.63 for particles of $<3.3\text{-}\mu\text{m}$ radius and $s = 4.96$ for particles $>3.3\text{-}\mu\text{m}$ radius. To explore the effect of changing the size distribution on the volume scattering function, we will use the proportional-shell (5%) model. The solid line in Fig. 11 is the volume scattering function obtained with this model for the central gyre chlorophyll maximum. For samples from the surface mixed layer, the PSD exponents were 2.97 and 5.41 for the small and large particles (Kitchen and Zaneveld 1990), while for samples from 125-m depth the exponents were 3.92 and 4.96. Two constant-exponent models of particle size distribution are also shown, with $s = 3.5$ and 6. These values are extremes for single-exponent models.

Except for the $s = 6$ model, changes in size distribution affect the shape of the volume scattering function much less than

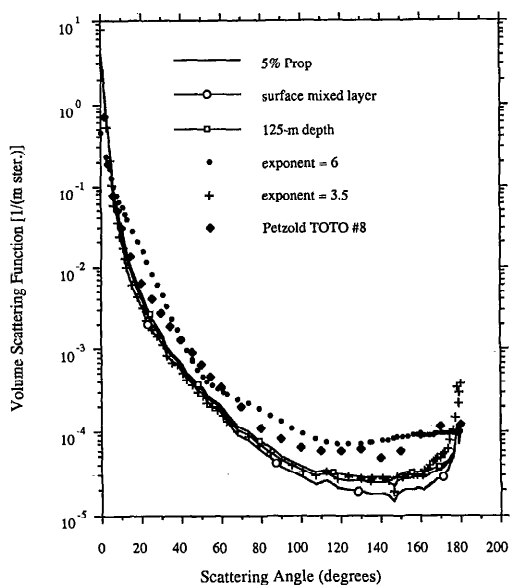


Fig. 11. The effect of changing the particle size distribution on the computed volume scattering functions for the model of 5% proportional shell thickness (with parameters from the fluorescence maximum). Results with observed size distributions from the central gyre mixed layer, fluorescence maximum, and 125-m depth are compared along with two uniform exponential distributions. Also shown is a measured particulate volume scattering function from the central gyre (Petzold 1972) obtained by subtracting scattering from seawater filtered for 18 h through diatomaceous earth from the observed scattering function.

changes in the internal structure or changes in the index of refraction for homogeneous spheres. The $s = 3.5$ model differs significantly from the reference model only beyond 160° . The difference in size distributions between these two models is essentially all in the large particle region. Thus we find that the shape of the volume scattering function is insensitive to large particles except beyond 160° , as was shown in the earlier section on cumulative volume scattering functions. The much different volume scattering function for the $s = 6$ size distribution further demonstrates the importance of very small particles.

Location of pigment within the cell—From Fig. 5, we see little change in the absorption efficiencies as a function of changes in structure (except that the homogeneous hard particle was a more effective absorber). This observation contradicts the notion that phy-

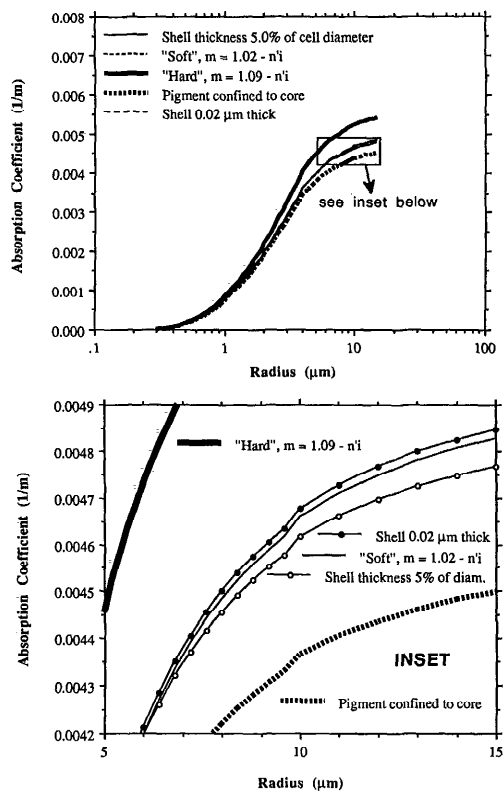


Fig. 12. The cumulative absorption coefficients relative to particle radius for three three-layered models and two homogeneous models of phytoplankton.

toplankton adjust their structure to maximize absorption; it also may contradict the so-called packaging effect (Morel and Bricaud 1981). To explore this further, we tried two extreme models—one with the pigment in the core and one with a very thin ($0.02 \mu\text{m}$) shell and the pigment confined to the middle layer. The cumulative absorption curves for these models are compared with the other models in Fig. 12. The model with the very thin shell differed insignificantly from the others, but the model with the pigment confined to the core showed a moderate reduction in absorption efficiency. The larger effect of increasing the index of refraction of the cytoplasm leads one to wonder whether compacting the chloroplasts into a smaller area close to the shell might effectively increase the index of refraction for that layer. This positive effect of the index of refraction on absorption can be un-

derstood from a geometrical optics point of view. An increased index of refraction would diminish the reflective losses between the shell and the chloroplasts, bending the light rays toward the center of the particle and increasing the pathlength of rays through the chloroplasts.

Conclusions

We have seen that including the effect of high-index-of-refraction outer shells in optical models of natural phytoplankton populations increases scattering at all angles except the very near-forward by more than one order of magnitude. Furthermore, the concentric models produced realistic volume scattering functions and attenuation coefficients even with only crude representations of internal structure dimensions. Thus, it is not necessary to have a high percentage of minerallike particles or very high concentrations of submicron particles to match the observed inherent optical properties in the central gyre.

The general shape and magnitude of the volume scattering function can be matched by polydispersions of three-layered spheres with a low-index-of-refraction interior and a medium-index shell. The forward scattering shows an excellent match between the three-layered model and historical data. Only the fine detail of the backscattering is not reproduced. That the fine detail of backscattering is not reproduced is not surprising given the large number of particle shape and structure characteristics that have been shown to affect backscattering. The present model thus shows promise for studying the optical effects of structural characteristics common to most classes of phytoplankton. The three-layered model can be applied on a desk-top computer; our study was done with a Macintosh II. We are encouraged by the usefulness of this method for studying the sensitivity of various optical parameters to phytoplankton characteristics.

Initial results show that knowledge of the wall-thickness distribution is critical to the details of the volume scattering function in the backward direction and that a scattering meter measuring from 3° to 6° could be expected to produce results correlating well with total scattering.

We did not observe a strong effect on absorption by phytoplankton as a function of internal structure. The lack of a strong effect on absorption seems reasonable because we required that the chlorophyll concentration for each size of cell remain constant from one model to another. This rearranging of pigment within the cell is different from the packaging effect described by Morel and Bricaud (1981), which was a comparison of absorption by particulate matter as a function of size and the imaginary part of the index of refraction. They found that the absorption peaks of chlorophyll were flattened for larger particles and higher complex indices. The small particles were more efficient absorbers in the Morel and Bricaud (1981) case because they had a smaller optical pathlength and thus less internal self-shading.

We have observed a shift to smaller average particle size with depth in the central gyre and reported on the optical implications elsewhere (Kitchen and Zaneveld 1990). Here we are interested in rearrangements of the chloroplasts within the cell, presumably in response to differing light conditions. Note that since we maintain the same total chlorophyll content per cell, the optical pathlength for absorption is not appreciably changed by compacting chlorophyll closer to the surface of the cell.

It may be that the cells also adjust the distribution of the real part of the index of refraction within the cell. The effect of varying the real part of the index of refraction as a function of location within the cell requires more study. We also need more information on the actual physical characteristics of phytoplankton cells as a function of cell size. When this information is obtained, we envisage that a wealth of understanding will come from further use of the three-layered-sphere model.

References

- AAS, E. 1981. The refractive index of phytoplankton. Univ. Oslo Rep. Ser. 46. 61 p.
- ASANO, S., AND M. SATO. 1980. Light scattering by randomly oriented spheroidal particles. *Appl. Opt.* 19: 962-974.
- BOHREN, C. F., AND D. R. HUFFMAN. 1983. Absorption and scattering of light by small particles. Wiley.

- BROWN, O. B., AND H. R. GORDON. 1973. Two component Mie scattering models of Sargasso Sea particles. *Appl. Opt.* **12**: 2461-2471.
- CHARNEY, E., AND F. S. BRACKETT. 1961. The spectral dependence of scattering from a spherical alga and its implication for the state of organization of the light-accepting pigments. *Arch. Biochem. Biophys.* **92**: 1-12.
- COHEN, L. D., R. D. HARACZ, A. COHEN, AND C. ACQUISTA. 1983. Scattering by light from arbitrarily oriented finite cylinders. *Appl. Opt.* **22**: 742-748.
- DOWNING, J. P., R. W. STERNBERG, AND C. R. B. LISTER. 1981. New instrumentation for the investigation of sediment suspension processes in the shallow marine environment. *Mar. Geol.* **42**: 19-34.
- GIBBS, R. J. 1978. Light scattering from particles of different shapes. *J. Geophys. Res.* **83**: 501-502.
- GORDON, H. R., AND OTHERS. 1988. A semianalytic radiance model of ocean color. *J. Geophys. Res.* **93**: 10,909-10,924.
- , AND A. MOREL. 1983. Remote assessment of ocean color for interpretation of satellite visible imagery. Springer.
- KERKER, M. 1969. The scattering of light and other electromagnetic radiation. Academic.
- KITCHEN, J. C., AND J. R. V. ZANEVELD. 1990. On the non-correlation of the vertical structure of light scattering and chlorophyll *a* in case 1 waters. *J. Geophys. Res.* **95**: 20,237-20,246.
- LATIMER, P. 1984. Light scattering by a structured particle: The homogeneous sphere with holes. *Appl. Opt.* **23**: 1844-1847.
- MEYER, R. A. 1979. Light scattering from biological cells: Dependence of backscatter radiation on membrane thickness and refractive index. *Appl. Opt.* **18**: 585-588.
- MIE, G. 1908. Beiträge zur Optik trüber Medien, speziell kolloidalen Metall-lösungen. *Ann. Phys.* **25**: 377.
- MOREL, A. 1988. Optical modeling of the upper ocean in relation to its biogenous matter content (case 1 waters). *J. Geophys. Res.* **93**: 10,749-10,768.
- , AND Y.-H. AHN. 1990. Optical efficiency factors of free-living marine bacteria: Influence of bacterioplankton upon the optical properties and particulate organic carbon in oceanic waters. *J. Mar. Res.* **48**: 145-175.
- , AND A. BRICAUD. 1981. Theoretical results concerning light absorption in a discrete medium, and application to the specific absorption of phytoplankton. *Deep-Sea Res.* **28**: 1375-1393.
- , AND L. PRIEUR. 1977. Analysis of variations in ocean color. *Limnol. Oceanogr.* **22**: 709-722.
- MUELLER, J. L. 1974. The influence of phytoplankton on ocean color spectra. Ph.D. thesis, Oregon State Univ. 239 p.
- PETZOLD, T. J. 1972. Volume scattering functions for selected ocean waters. Univ. Calif. Scripps Inst. Oceanogr. Ref. 72-28.
- PLATT, T., S. SATHYENDRANATH, C. M. CAVERHILL, AND M. R. LEWIS. 1988. Ocean primary production and available light: Further algorithms for remote sensing. *Deep-Sea Res.* **35**: 855-879.
- QUINBY-HUNT, M. S., A. J. HUNT, K. LOFFTUS, AND D. SHAPIRO. 1989. Polarized-light scattering studies of marine *Chlorella*. *Limnol. Oceanogr.* **34**: 1587-1600.
- STRAMSKI, D., AND D. A. KIEFER. 1991. Light scattering by microorganisms in the open ocean. *Prog. Oceanogr.* **28**: 343-383.
- ZANEVELD, J. R. V., D. M. ROACH, AND H. PAK. 1974. The determination of the index of refraction distribution of oceanic particulates. *J. Geophys. Res.* **79**: 4091-4095.

Submitted: 20 December 1991

Accepted: 13 May 1992

Revised: 28 July 1992